Supplemental Materials for

Quantifying new versus old PM deposition in forest canopies: new throughfall mass balance with fallout radionuclide chronometry

Joshua D. Landis[1]

[1]Dartmouth College, 19 Fayerweather Hill Road, Hanover NH 03755 USA
correspondence to joshua.d.landis@dartmouth.edu

S1. Supplemental Methods

S1.1. Preconcentration of FRNs from throughfall precipitation

FRNs in the acidified filtrate were preconcentrated by MnO_2 co-precipitation to determine an operationally-dissolved fraction as follows. The acidified filtrate was first spiked with 500 µg ^{9}Be and 250 µg stable Pb yield monitors, and a 20 mL aliquot removed (*a1*). The filtrate was then co-precipitated with MnO_2 by adding sequentially NH_4OH to bring pH to ~9 (3% v/v), 15 μmol $MnCl_2$ and 70 or 280 μmol $KMnO_4$ to openfall or throughfall samples. Higher amounts of $KMnO_4$ are needed for throughfall samples due to the consumption of oxidizing capacity by dissolved organic carbon (DOC). After 24 hours flocculation the MnO_2 precipitate was filtered to quartz fiber (QF) filters. A second aliquot (*a2*) was taken from the filtrate and Be and Pb were measured in both *a1* and *a2* aliquots by inductively-coupled plasma optical emission spectroscopy (ICPOES). Be and Pb yields were then calculated as (*a*1-*a*2)/*a*1 x100%, averaging 88 ±15% for Be and 88 ±16% for Pb (mean ±SD).

Following deployment, collectors were first rinsed in deionized water (DI), scrubbed with cellulose wipes, rinsed 5x in DI, scrubbed with Citranox detergent using a plastic-bristle brush, rinsed 25x and then filled to overflowing with DI. The full collectors were then allowed to sit for a minimum of 7 days before reuse, at which time they were emptied and rinsed a further 10x in DI. Process blanks were routinely measured by deploying collectors, immediately retrieving, and processing them as for samples, and all data are corrected as necessary.

S1.2. Composition and canopy interactions of throughfall

We collected paired openfall (*W*) and throughfall samples (*T*) at either BM or SO sites during 52 storms in the years 2018-2022. Of these, 22 storms were collected at both BM and SO sites. Two trees were sampled per site for a grand total of 156 throughfall measurements. These represented all seasons and precipitation totals ranging from 0.05 to 7.0 cm (geometric mean, GM =1.52 cm). The higher elevation BM site recorded about 5% more openfall precipitation than the SO site but the difference was not significant [p=0.34]. The fraction of precipitation intercepted by the canopy decreased with increasing precipitation (Fig. S1). Stemflow was not measured in this study but typically contributes ca. 5% of total throughfall volume. Annual throughfall interception for each species decreased as follows for the leaf-on seasons: spruce (30%) < pine (24%) < SO oak (23%) < BM oak (13%). Spruce retained a greater fraction of incident precipitation due to either higher LAI, canopy architecture, or some combination thereof.

S1.3. FRN and MTE speciation: implications for collection protocols

We distinguished three operational fractions in MTE open and throughfall deposition, an operationally-dissolved water-soluble fraction (*d*.), a weak-acid soluble fraction (*s*.) measured by extracting FPOM

filters in 2% HCl, and a refractory fraction that is incorporated in particulate matter (*r*.) and measured by aqua regia extraction of filters. Throughfall collections are typically analyzed only for a water-soluble fraction of MTEs, e.g., Gandois et al., 2010; Hou et al., 2005; Lindberg & Harriss, 1981; Lovett & Lindberg, 1984; Anne W. Rea et al., 2001. Our new protocol provides an operational means of separating long-range aerosols, which are highly soluble, from locally resuspended dust, which is typically insoluble, e.g., Fishwick et al., 2017. This approach also allows further speciation of MTEs by, e.g., filtration or ultrafiltration (Gandois et al., 2010; Hou et al., 2005). In prior approaches samples are acidified for preservation only after filtration or separation from the collector and any particulate fraction.
In contrast, FRNs are typically measured following acidification since this is required to recover total deposition of particle-reactive metals (Baskaran et al., 1993). Our previous work with FRNs in bulk atmospheric deposition shows that up to 100% of total ^{7}Be or ^{210}Pb activity may be found in the >0.5 µm fraction (median 23% and 55%, respectively), depending on the mass concentration of total particulate matter (p_C) as well as pH and the presence of Mn, Al, and Fe oxides or surface coatings that drive FRN sorption to the particulate fraction (Landis et al., 2021). The FRN activity-fraction particulate (f_P) also increases with aerosol age in what we call a particle age effect (p.a.e.). We previously determined that 20-30% of FRN activity is lost from bulk precipitation if the sample collection train is not rinsed with 2% HCl to recover FRNs that sorb to collector walls (Landis et al., 2021). For these reasons we believe it imperative to measure both operationally dissolved (*d*.Al, etc.), acid-soluble (*s*.Al, etc.) and refractory (*r*.Al, etc.) fractions since many MTEs of interest are, like the FRNs, particle- and surface-reactive.
Here the *s*. and *t*. fractions were measured following sample filtration by extraction of quartz fiber filters. QFF filters were extracted sequentially, first using 50 mL 2% HCl. The supernatant from this step was separated by centrifugation as the *s.* fraction, and filters then digested using 12 mL reverse aqua regia (3:1 HNO_3:HCl, Optima grade) with addition of 2% v/v BrCl. Digests were allowed to react at room temperature for 15 hours and were then diluted by addition of 30 mL 2% HCl. Final solutions were measured by ICPOES for major elements, ICPMS for trace metals, and purge-and-trap fluorescence for Hg.

Recovery of total FRN activity by 2% HCl was previously established for bulk deposition (Landis et al., 2021). To assess the recovery of FRNs by 2% HCl in throughfall we followed 6 collections with a 6N HCl rinse; these were aggregated to improve detection limits and then pre-concentrated by MnO_2 precipitation. The aggregate yield in the rinse was equivalent to 0.4 ±0.2% of total ^{7}Be and 1.4 ±0.4% of total ^{210}Pb, indicating near-complete recovery of FRNs by 2% HCl.

S1.4. Partitioning coefficients and behavior of ^{7}Be and ^{210}Pb in throughfall

We use partitioning metrics to assess the solubility behaviors of FRNs and MTEs. We calculate the equilibrium partitioning or distribution coefficient (K_D) as follows:

$$K_D = \frac{A^{>0.5}/M}{A^{<0.5}/V} = \frac{A^{>0.5}}{A^{<0.5} \cdot p_C} \qquad \text{Eq. S1}$$

We calculate the activity-fraction particulate according to the following, since at low particulate concentrations a large proportion of FRN activity may remain operationally-dissolved despite K_D values exceeding 10^5 (Landis et al., 2021b):

$$f^{Be} \text{ or } f^{Pb}\,(\%) = \frac{A^{>0.5}}{A^{>0.5} + A^{<0.5}} \times 100 \qquad \text{Eq. S2}$$

We note that f_P is explicitly related to the product $K_D \cdot p_C$ as follows:

$$f_P = 1 - \frac{1}{1+K_D \cdot p_C} \qquad \text{Eq. S3}$$

For both ^{7}Be and ^{210}Pb, $\log_{10}(K_D)$ is significantly lower in TF than in OF. For ^{7}Be, corresponding $\log_{10}(K_D)$ values were 3.86 ±0.05 and 4.55 ±0.07 (mean ±SE), respectively, a decrease by a factor of 5 in TF [p<0.0001]. Corresponding $\log_{10}(K_D)$ for ^{210}Pb in TF and OF were 4.24 ±0.05 and 5.17 ±0.08, a decrease by a factor of 9 in TF[p<0.0001]. At each site the ^{7}Be $\log_{10}(K_D)$ for pine or spruce is significantly lower than oak, but this is not the case for ^{210}Pb [p>0.05]. All species and sites show a significant decrease in $\log(K_D)$ with $\log(p_C)$ for both ^{7}Be and ^{210}Pb, a particle concentration effect (p.c.e.) indicating that FRN solubility is controlled by colloidal phases (Landis et al., 2021) (Fig. S7). This suggests that the speciation of ^{7}Be and ^{210}Pb may be modified in transit through the canopy through sorption to the canopy and complexation by DOC (Gandois et al., 2010; Hou et al., 2005). When corrected for p.c.e using linear regression against $\log(p_C)$, however, there is no difference in ^{7}Be $\log_{10}(K_D)$ in TF versus OF [$t(217)$=-0.32, p=0.75]. That is, the reduction in ^{7}Be K_D in throughfall is attributable to the p.c.e. In contrast, for ^{210}Pb $\log_{10}(K_D)$ in TF is significantly lower than OF [$t(217)$=-3.3, p=0.0013]; this suggests that ^{210}Pb may be solubilized by DOC during residence in the canopy.

S2. Throughfall Chemistry

Precipitation chemistry was modified during transit through the canopy, with DOC increasing from 0.7 mg L^{-1} in OF to 9.2 mg L^{-1} in TF (geometric means, GM). DOC was lowest in winter but not different among spring, summer, or autumn [p<0.05]. Mass concentration of fine particulate organic matter (FPOM 0.5 um to 1 mm diameter, hereafter p_C) similarly increased from 2.6 ±0.5 mg L^{-1} to 21 ±3 mL^{-1} in throughfall (GM ±SE). p_C and DOC were strongly, linearly correlated [R^2=0.55, p<0.0001, n=156]. We used multiple regression to identify factors influencing total FPOM loading from the canopy. The effect of each independent factor was quantified as $e*$, which is the percent of total variance in the response variable that is explained by each independent explanator. Total FPOM flux per unit area (m_D) was strongly seasonal with a summer maximum [$e*$=26%, p<0.0001], but also driven by increasing p_D [15%, p<0.0001] and longer antecedent dry periods [10%, p=0.0003]. Seasonal FPOM concentrations increased in the order: winter (8 ±4 mg L^{-1})^B < spring (13 ±3)^B < autumn (16 ±3)^B < summer (47 ±9)^A. A p_D threshold =15 mm to define the antecedent period yielded a stronger effect than either 5 mm or 1 mm, indicating that substantial precipitation is needed to remove susceptible FPOM from the canopy, or that longer periods are required for FPOM to accumulate. There were no differences in p_C by species [p=0.092] or site [p=0.62], In contrast to FPOM, export of DOC from the canopy showed no dependence on antecedent period. Significant multiple regression explanators for DOC included season [24%], p_D [10%] and species [5%].

Effect of the canopy on throughfall pH was variable (Fig. S2). The canopy was a net sink for H^+ in summer for each of spruce, pine and oak [p<0.05]. On an annual basis, oak was a net sink at both sites but both pine and spruce were net sources of H^+. Corrected for seasonality, H^+ yields increase in the order: BM oak (44%)^C < SO oak (86%)^{BC} < BM pine (111%)^{AB} < SO spruce (180%)^A [GMs; values connected by the same letter were not different, p<0.05]. Corrected for the species effect, throughfall yield of H^+ was significantly lower in autumn and summer: summer (-96%)^A < autumn (-92%)^A < spring (81%)^B < winter (104%)^B. Throughfall mean pH values for the seasons were 5.29, 5.36, 4.98, and 4.86, respectively.

The observed behavior of metals in throughfall can be assessed with the partition coefficient K_D, which quantifies the affinity of metals for particulate matter versus operationally dissolved fraction. Consistent with earlier observations (Landis et al. 2021b), we observe that ^{7}Be has lower K_D than ^{210}Pb (Fig. S7). For both ^{7}Be and ^{210}Pb throughfall has lower K_D than openfall precipitation, at both sites and all trees studied here. This implies that DOC in throughfall plays an important role in modifying PM metal speciation. The stable isotope counter parts to the FRNs, ^{9}Be and Pb, provide important context to these measurements for the FRNs. The stable isotopes similarly show higher K_D in openfall versus throughfall. While we observe that stable Pb has comparable K_D to ^{210}Pb, at the same time ^{9}Be has significantly higher K_D than ^{7}Be or indeed than either Pb isotope. We interpret this as evidence of a particle age effect (p.a.e.) whereby the strength of partitioning to a particulate phase increase with the lifetime of the metal in recirculation within the ecosystem.

We constructed multiple regression correlation webs for $\log_{10}(K_D)$ to illustrate the factors that influence partitioning of the FRNs. Multiple regressions are shown in Fig. S8. We began modeling by including environmental factors: season, species, site, pH, log(FPOM*)*, log(preciptitation), and antecedent dry period. For ^{7}Be log(K_D) the general model explains 84% of variance [R^2=0.84, n=100, p<0.0001]. Explanators log(FPOM) [61%], season [5.1%], site [4.9%], species [4.7%], pH [4.2%], and log(preciptitation) [2.7%] all contributed significant independent effects. Antecedent dry period did not [p=0.72]. The general model for ^{210}Pb log(K_D) was similarly strong [R_a^2=0.78, p<0.0001] with significant effects from log(FPOM) [47%], log(precipitation) [9%], pH [11%], and season [12%]. There were no effects from antecedent [p=0.70] or species [p=0.32]. Adding log(DOC) [5.8%] superceded both pH and seasonal effects. The importance of pH in ^{210}Pb partitioning in throughfall is a notable departure from its behavior in bulk openfall where no correlation was found for ^{210}Pb (Landis et al., 2021).

From a mass-balance perspective, we stress that while $\log_{10}(K_D)$ is substantially lower in throughfall, the total fraction of ^{7}Be and ^{210}Pb activities found in the particulate fraction (f^{Be} and f^{Pb}) are either unchanged for ^{210}Pb or actually higher for ^{7}Be in TF over incident OF. This occurs because decreases in K_D are offset by the large mass of FPOM derived from the canopy. f_{Be} increased from 8.7 ±1.1% to 13.7 ±1.0% from openfall to throughfall while f_{Pb} was unchanged from 33±2% to 32±2%.

S3. Bias of conventional mass balance in trace metal cycles

To explain divergence between multiple-regression and filtering mass balance approaches, we review the implicit assumptions in each. The filtering approach assumes that the reference element has no leaching or metabolic contributions. This assumption has been challenged for both Na (Wyttenbach and Tobler, 1988) and Al (Rehmus et al., 2017), and indeed ecosystem mass balances have demonstrated that essentially all trace metals show some degree of metabolic assimilation into long-lived tissues of the tree (Bergkvist, 1987; Landre et al., 2009). The filtering approach further assumes implicitly that apportioning of deposition between wet and dry processes is identical for both reference and target elements. This in turn requires identical aerosol size distributions and thus aerosol sources *vis a vis* secondary aerosol or recycled dust since the removal processes of 1 um versus 10 um aerosols are quite different (Jaenicke, 1980). Deposition of crustal elements such as Al, with low concentrations in rainwater and high concentrations in dust, is dominated by dust (Landis et al., 2021). In filtering mass balance, if the reference element is influenced by either canopy leaching (Na) or resuspended dust (Al), the result will overestimate dry deposition for secondary aerosols like ^{7}Be and ^{210}Pb or other metals in long-range transport.

TMs are typically assumed atmospheric in origin, e.g., Lovett & Lindberg (1984), so the role of resuspended dust in TF is important to resolve since it might create large throughfall EFs without providing new TM deposition. Moreover, soils store enormous reservoirs of legacy pollutants such as Pb and Hg bound to both organic and mineral particles. These larger dust particles (10-100 µm) have lower solubility than secondary aerosol (<1µm) due to different mineralogy, composition, and surface area (Fishwick et al., 2017). Thus, while secondary aerosol dry deposition may be highly soluble and efficiently rinsed from the canopy, dust particles may require long residence times to be solubilized by production of DOC within the phyllosphere. This process would explain strong DOC associations of Be^T, Pb^T, Al, and Fe in throughfall.

In the multiple regression approach, it is assumed that antecedent dry deposition is fully removed by each rainstorm and incorporated into throughfall (Lovett and Lindberg, 1984). If some fraction of dry deposition remains stored in the canopy (no steady-state at the event scale), the multiple regression antecedent coefficient (β_1) will underestimate dry deposition. This approach may also fail to record the influence of dust deposition if dust constituents are either strongly retained or rapidly removed relative to fine PM. Dry dust deposition may be released subsequently in conjunction with higher rainfall totals and larger fluxes of DOC, as we observe here with TMs in throughfall. In sum, the biases in each mass balance method can lead their results to diverge. While the filtering approach grossly overestimates deposition of secondary aerosols as shown here with FRNs, it may be better suited for conservative species, e.g., NO_3, that do not interact and sorb strongly to the canopy as metals do.

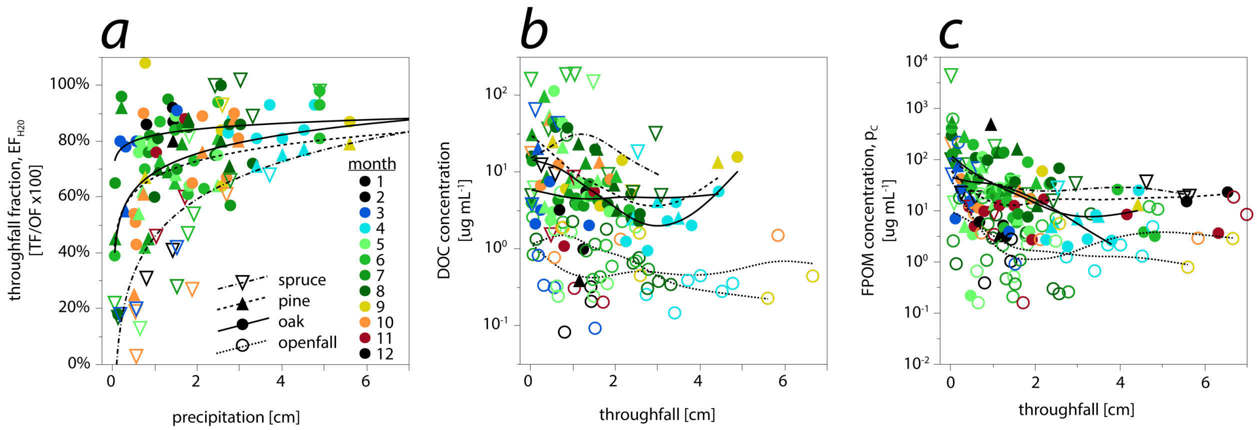

Figure S1. precipitation interaction with tree canopy, (a) interception, (b) DOC concentrations of throughfall, (c) FPOM concentrations.

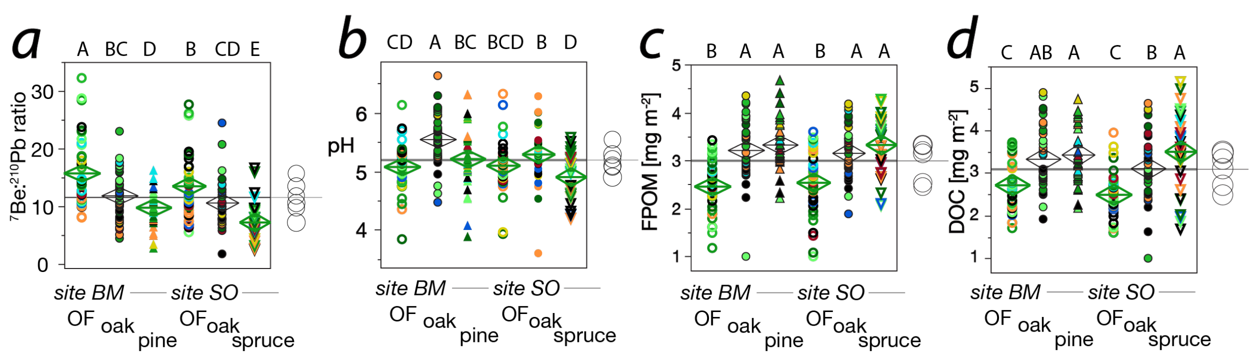

Figure S2. species effects in throughfall on (a) ^7Be:^{210}Pb, (b) pH, (c) FPOM, (d) DOC.

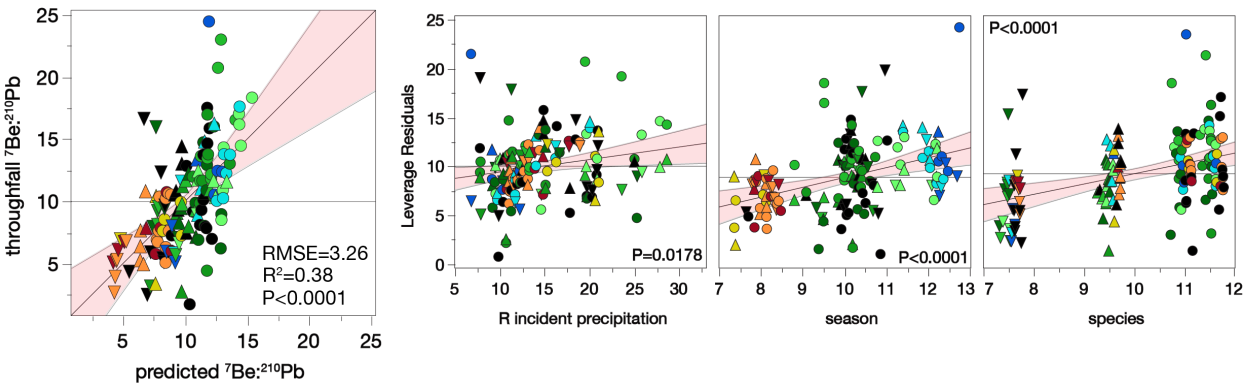

Figure S3. multiple regression for ^{7}Be:^{210}Pb ratios in throughfall. Larger panel shows overall model fit and smaller panels show leverage of individual explanators.

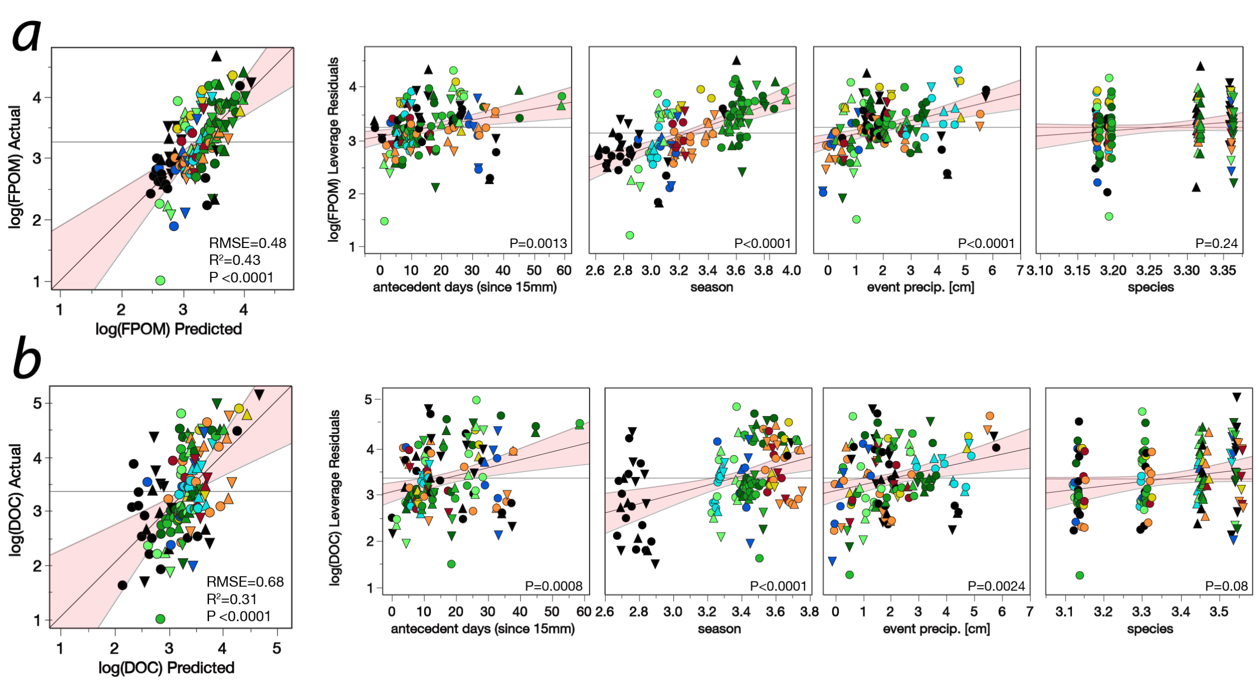

Figure S4. multiple regression for (a) FPOM and (b) DOC fluxes in throughfall. Larger panels show overall model fit and smaller panels show leverage of individual explanators.

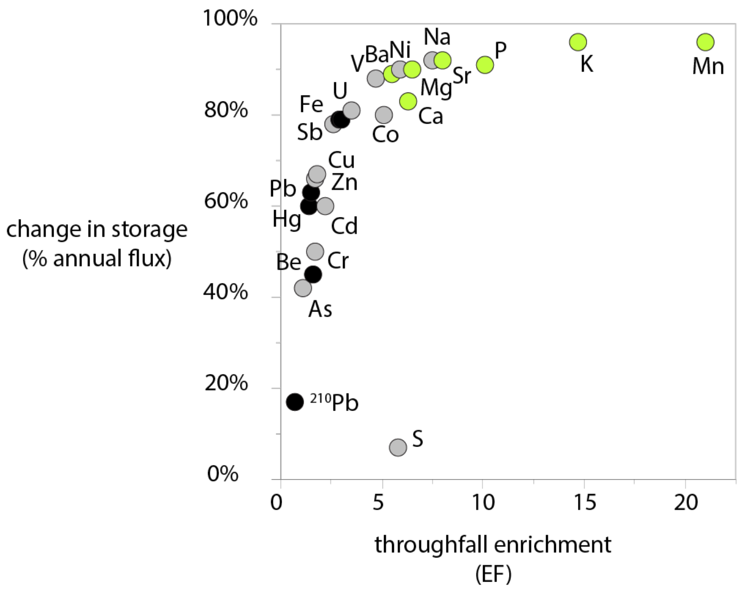

Figure S5. relationship of change in storage to throughfall enrichment for major and trace elements. Note divergence of sulfur which has high EF despite low change in storage due to dry deposition of gaseous SO_2.

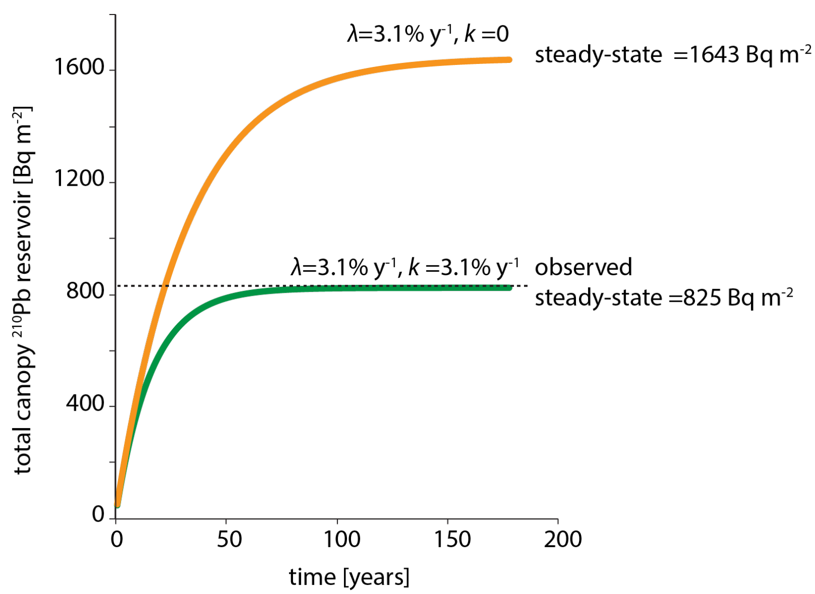

Figure S6. modeling of ^{210}Pb ingrowth for whole-tree canopy with measured wet+dry inputs, minus throughfall and annual litter export. Total year-on-year gain to the canopy totals 51 Bq m^{-2} y^{-1} (Landis 2024). Cases are considered for (1) only radioactive decay (orange) and (2) decay plus physicochemical weathering (green). A loss constant k=3.1% y^{-1} predicts the observed whole-tree inventory of 825 Bq m^{-2} with a corresponding loss of 25 Bq m^{-2} y^{-1} through weathering of the canopy.

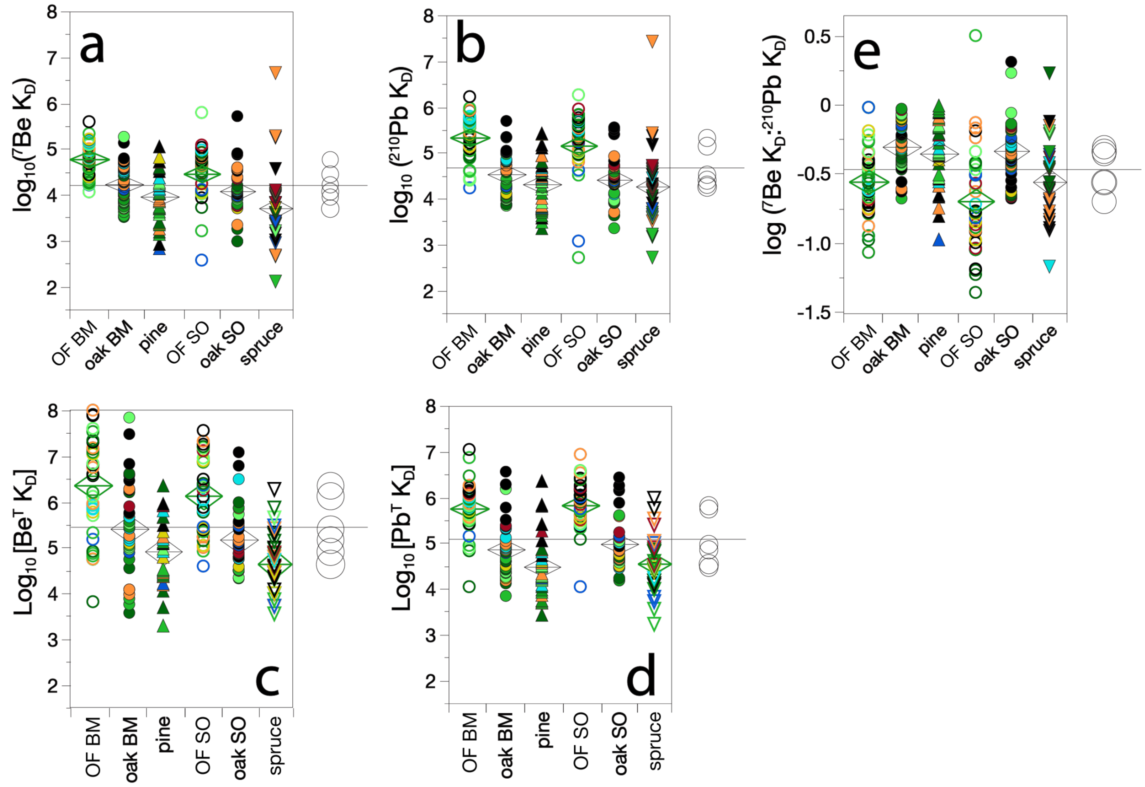

Figure S7. partition coefficients (K_D) for (a) ^{7}Be and (b) ^{210}Pb, their ratio (c), and (d) Be^T and (e) Pb^T. While ^{7}Be typically has a lower K_D than ^{210}Pb, the stable isotope ^{9}Be has higher K_D than observed for either ^{210}Pb or stable Pb. This may indicate a change in speciation with time of PM in circulation (i.e., particle age effect).

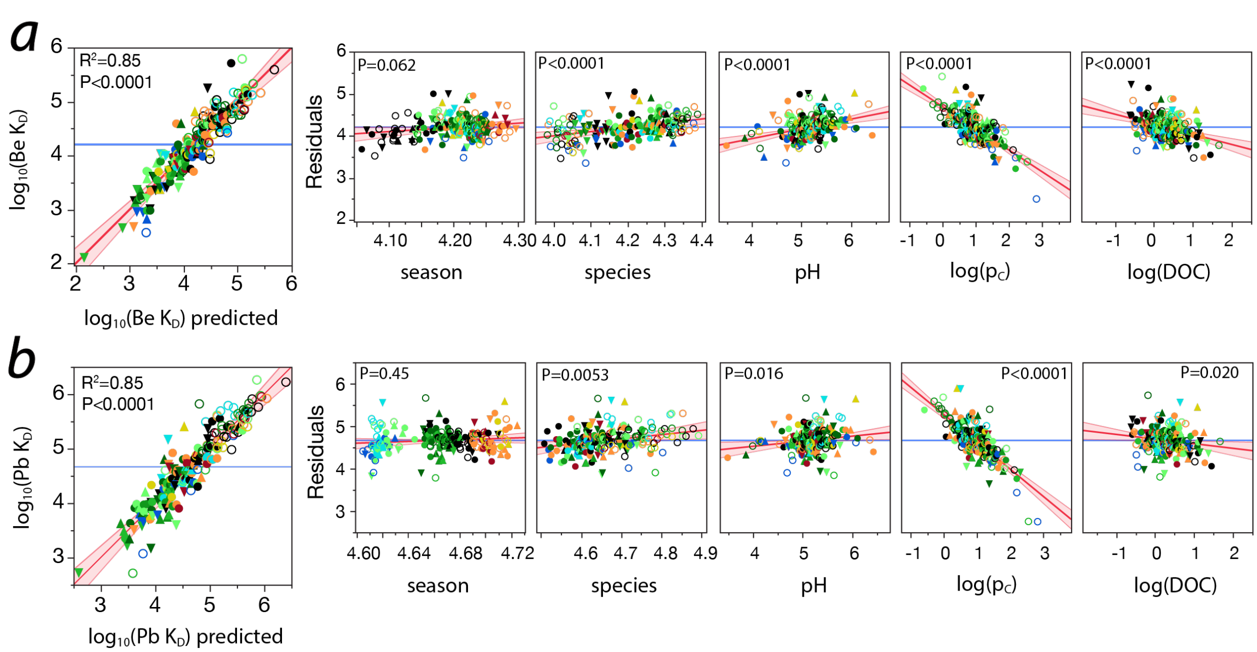

Figure S8. multiple regression for (a) ^{7}Be and (b) ^{210}Pb partition coefficients (K_D).

References

Baskaran, M., Coleman, C. H., and Santschi, P. H.: Atmospheric Depositional Fluxes of Be-7 and Pb-210 at Galveston and College-Station, Texas, Journal of Geophysical Research-Atmospheres, 98, 20555–20571, https://doi.org/Doi 10.1029/93jd02182, 1993.

Bergkvist, B. O.: Soil solution chemistry and metal budgets of spruce forest ecosystems in S. Sweden, Water Air Soil Pollut, 33, 131–154, 1987.

Fishwick, M. P., Ussher, S. J., Sedwick, P. N., Lohan, M. C., Worsfold, P. J., Buck, K. N., and Church, T. M.: Impact of surface ocean conditions and aerosol provenance on the dissolution of aerosol manganese, cobalt, nickel and lead in seawater, Mar Chem, 198, 28–43, https://doi.org/10.1016/j.marchem.2017.11.003, 2017.

Gandois, L., Tipping, E., Dumat, C., and Probst, A.: Canopy influence on trace metal atmospheric inputs on forest ecosystems: Speciation in throughfall, Atmos Environ, 44, 824–833, https://doi.org/10.1016/j.atmosenv.2009.11.028, 2010.

Hou, H., Takamatsu, T., Koshikawa, M. K., and Hosomi, M.: Trace metals in bulk precipitation and throughfall in a suburban area of Japan, Atmos Environ, 39, 3583–3595, https://doi.org/10.1016/j.atmosenv.2005.02.035, 2005.

Jaenicke, R.: Natural Aerosols, Ann N Y Acad Sci, 338, 317–329, https://doi.org/10.1111/j.1749-6632.1980.tb17129.x, 1980.

Landis, J. D., Feng, X., Kaste, J. M., and Renshaw, C. E.: Aerosol populations, processes and ages contributing to bulk atmospheric deposition: insights from a 9-year study of 7Be, 210Pb, sulfate and major/trace elements, Journal of Geophysical Research: Atmospheres, 2021a.

Landis, J. D., Renshaw, C. E., and Kaste, J. M.: Sorption Behavior and Aerosol-Particulate Transitions of7Be,10Be, and210Pb: A Basis for Fallout Radionuclide Chronometry, Environ Sci Technol, 55, 14957–14967, https://doi.org/10.1021/acs.est.1c03194, 2021b.

Landre, A. L., Watmough, S. A., and Dillon, P. J.: The effects of dissolved organic carbon, acidity and seasonality on metal geochemistry within a forested catchment on the Precambrian Shield, central Ontario, Canada, Biogeochemistry, 93, 271–289, https://doi.org/10.1007/s10533-009-9305-0, 2009.

Lindberg, S. E. and Harriss, R. C.: The role of atmospheric deposition in an eastern U.S. deciduous forest, Water Air Soil Pollut, 16, 13–31, 1981.

Lovett, G. M. and Lindberg, S. E.: Dry Deposition and Canopy Exchange in a Mixed Oak Forest as Determined by Analysis of Throughfall, J Appl Ecol, 21, 1013, https://doi.org/10.2307/2405064, 1984.

Rea, A. W., Lindberg, S. E., and Keeler, G. J.: Dry deposition and foliar leaching of mercury and selected trace elements in deciduous forest throughfall, Atmos Environ, 35, 3453–3462, https://doi.org/10.1016/S1352-2310(01)00133-9, 2001.

Rehmus, A., Bigalke, M., Boy, J., Valarezo, C., and Wilcke, W.: Aluminum cycling in a tropical montane forest ecosystem in southern Ecuador, Geoderma, 288, 196–203, https://doi.org/10.1016/j.geoderma.2016.11.002, 2017.

Wyttenbach, A. and Tobler, L.: The seasonal variation of 20 elements in 1st and 2nd year needles of Norway spruce, Picea abies (L.) Karst, Trees, 2, 52–64, https://doi.org/10.1007/BF01196345, 1988.=

Table S1: throughfall and crustal enrichment for FRNs and MTEs*

		log($EF_{crustal}$)	EFcrustal	***d.*** **W**	***d.*** **T**	**d.EF**	***s*** **.W**	***s*** **.T**	**s.EF**	***t*** **.W**	***t*** **.T**	**t.EF**	**Δ*S***	***new***
				ug m^{-2} y^{-1}	ug m^{-2} y^{-1}		ug m^{-2} y^{-1}	ug m^{-2} y^{-1}		ug m^{-2} y^{-1}	ug m^{-2} y^{-1}		%	%
^{7}Be	Bq m^{-2}	6.43	2.7E+06	1479	730	0.49				1647	873	0.53		100%
^{210}Pb	Bq m^{-2}	4.43	2.7E+04	86	64	0.74				126	92	0.73	29%	71%
Hg^{T}	ug m^{-2}	3.70	5.0E+03	4.9	5.3	1.1	5.0	5.4	1.1	6.9	10.0	1.45	60%	40%
Al	ug m^{-2}	0.00	1.0E+00	3834	22769	5.9	10305	36185	3.5	29829	85620	2.87	79%	21%
As	ug m^{-2}	3.78	6.1E+03	181	175	1.0	188	188	1.0	204	223	1.09	42%	58%
Ba	ug m^{-2}	1.88	7.5E+01	818	3981	4.9	958	4782	5.0	1047	5800	5.54	89%	11%
^{9}Be	ug m^{-2}	1.09	1.2E+01	0.7	1.8	2.4	3.0	4.5	1.5	3.5	5.6	1.58	45%	55%
Ca	ug m^{-2}	2.27	1.8E+02	109434	697193	6.4	119775	756769	6.3	123469	775106	6.28	83%	17%
Cd	ug m^{-2}	3.65	4.5E+03	9	18	2.1	9	21	2.2	10	22	2.24	60%	40%
Co	ug m^{-2}	2.06	1.2E+02	23	150	6.6	28	165	5.8	39	199	5.10	80%	20%
Cr	ug m^{-2}	2.31	2.0E+02	141	177	1.3	149	200	1.3	188	317	1.68	50%	50%
Cu	ug m^{-2}	3.31	2.0E+03	1000	1795	1.8	1198	2046	1.7	1287	2363	1.84	67%	33%
Fe	ug m^{-2}	0.77	5.9E+00	4054	15962	3.9	10824	32840	3.0	41923	124182	2.96	79%	21%
K	ug m^{-2}	2.21	1.6E+02	90706	2373294	26.2	95076	2409250	25.3	167142	2459673	14.72	96%	4%
Mg	ug m^{-2}	1.90	8.0E+01	21101	176857	8.4	24651	189503	7.7	33934	220638	6.50	90%	10%
Mn	ug m^{-2}	2.30	2.0E+02	2367	60124	25.4	2818	63515	22.5	3081	64766	21.02	96%	4%
Na	ug m^{-2}	2.17	1.5E+02	85129	643225	7.6	89498	679181	7.6	91059	683665	7.51	92%	8%
Ni	ug m^{-2}	2.83	6.8E+02	269	1747	6.5	294	1850	6.3	337	1985	5.89	90%	10%
P	ug m^{-2}	2.97	9.4E+02	13048	143860	11.0	15287	159135	10.4	17903	180792	10.10	91%	9%
Pb	ug m^{-2}	2.51	3.3E+02	129	310	2.4	342	499	1.5	373	562	1.51	63%	37%
S	ug m^{-2}	3.12	1.3E+03	110828	634776	5.7	111772	640567	5.7	114412	658797	5.76	7%	93%
Sb	ug m^{-2}	3.98	9.6E+03	38	102	2.7	43	106	2.5	49	125	2.58	78%	22%
Sr	ug m^{-2}	1.75	5.6E+01	386	3254	8.4	430	3513	8.2	451	3599	7.99	92%	8%
V	ug m^{-2}	2.58	3.8E+02	454	2309	5.1	529	2554	4.8	602	2806	4.66	88%	12%
U	ug m^{-2}	0.76	5.7E+00	0.3	2.1	6.5	0.8	2.6	3.2	1.3	4.7	3.48	81%	19%
Zn	ug m^{-2}	3.99	9.9E+03	13863	21171	1.5	14303	22681	1.6	15342	26828	1.75	66%	34%

*data are given for dissolved fraction (d.), weak acid soluble fraction (s.), and total (t.) which is the sum of d., s., and refractory (r.)
W represents event-based wet or openfall preciptation, T represents throughfall, EF is enrichment factor, S is change in storage

Table S2 Throughfall multiple regression mass balance estimates of dry deposition, absorption, and carbon association

	total deposition		β_1			β_2			D_β		C_β		β_{DOC}	K_{DOC}
	ug m^{-2} y^{-1}	R^2	ng m^{-2} d^{-1}	σ	*p*	ng cm^{-1}	σ	*p*	ug m^{-2} y^{-1}	%	ug m^{-2} y^{-1}	%	umol $umol^{-1}$	L $umol^{-1}$
^{7}Be	1860	0.45	0.58	0.15	0.008	-5.8	0.8	<.0001	213	11%	-987	-53%	1.44E-03	1.02E-03
^{210}Pb	145	0.22	0.053	0.015	0.001	-0.18	0.09	0.044	19	13%	-53	-37%	2.23E-04	1.84E-03
Hg^T	8	0.51	3.8	1.4	0.007	30	8	0.0004	1.4	17%	2	21%	1.98E-07	8.32E-03
Al	41024	0.53	30672	11	0.006	95	67	0.16	11195	27%	44596	109%	1.04E-02	2.87E-02
As	230	0.32	72	30	0.018	510	177	0.005	26.2	11%	-7	-3%	3.75E-06	1.39E-03
Ba	1048	0.62	2.3	1.0	0.023	27	5	0.023	0.8	0%	4752	454%	2.92E-04	4.31E-03
^{9}Be	5	0.49	3.4	1.1	0.003	16	7	0.003	1.2	26%	1	17%	3.25E-06	2.93E-02
Ca	318784	0.58	535110	128	<.0001	1490	722	0.041	195315.0	61%	456322	143%	1.01E-01	1.15E-02
Cd	13	0.47	9	3	0.008	11	19	0.57	3.3	26%	9	67%	3.52E-07	3.49E-03
Co	75	0.63	98	41	0.018	607	231	0.0097	35.8	48%	124	166%	4.24E-06	6.10E-03
Cr	233	0.57	123	48	0.012	123	48	0.0044	44.8	19%	84	36%	1.31E-05	4.41E-03
Cu	1837	0.48	1505	545	0.007	7245	3100	0.0210	549.5	30%	526	29%	7.50E-05	3.44E-03
Fe	60323	0.62	50410	16	0.005	91	94	0.33	18399.8	31%	63859	106%	1.00E-02	8.31E-02
K	713459	0.61	1496758	373	0.0001	7467	2035	0.0004	546316.6	77%	1746214	245%	4.07E-01	2.28E-02
Mg	33934												5.35E-02	1.60E-02
Mn	14216	0.67	30508	9235	0.001	173033	50133	0.0008	11135	78%	50550	356%	4.93E-03	4.67E-02
Na	120690	0.49	81181	69	0.24	458	397	0.2513	29630.9	25%	562975	466%	4.12E-02	6.71E-03
Ni	948	0.54	1674	595	0.006	6083	3380	0.0744	610.9	64%	1037	109%	8.14E-05	1.02E-02
P	40881	0.62	62953	25	0.012	549	134	<.0001	22977.9	56%	139911	342%	3.89E-02	3.37E-02
Pb	434	0.42	83	94	0.077	1749	605	0.0046	30.3	14%	128	30%	1.68E-05	2.04E-02
S	191696	0.66	212	0.075	0.006	1.4	0.4	0.0012	77284.3	40%	467101	244%	2.99E-02	4.56E-03
Sb	65	0.55	45	34	0.196	840	196	<.0001	16.3	25%	60	93%	1.69E-06	4.05E-03
Sr	452	0.54	3	1	0.001	8	6	0.17	1.3	0%	3147	697%	1.05E-04	7.61E-03
V	1170	0.61	1556	809	0.057	18435	4606	0.0001	568.0	49%	1636	140%	1.08E-04	3.50E-02
U	2	0.60	2	1	0.002	10	4	0.0276	0.9	39%	2	111%	7.61E-08	2.45E-02
Zn	21684	0.51	17375	5539	0.002	118576	31532	0.0003	6341.7	29%	5144	24%	9.44E-04	3.69E-03

*multiple regression with explanators season, species, antedent dry period, throughfall depth [cm], and DOC mass [log(mg m-2)].

Table S3: filtering mass balance of FRNs and MTEs with Al reference

	total ug m^{-2} y^{-1}	**D_{Al}** ug m^{-2} y^{-1}	**C_{Al}** ug m^{-2} y^{-1}	**EF**	**[M]** Bq or ng L^{-1}
^{7}Be	4727	3080	-3686	0.53	1.41
^{210}Pb	361	235	-229	0.73	0.121
Hg^{T}	20	13	-8	1.45	0.00475
Al	85620	55791	25995	2.87	8
As	585	381	-339	1.09	0.202
Ba	3005	1958	3024	5.54	1.8
^{9}Be	10	7	-2	1.58	0.001
Ca	354397	230928	434744	6.28	350
Cd	28	18	-5	2.24	0.0113
Co	112	73	103	5.10	0.041
Cr	541	352	-176	1.68	0.155
Cu	3694	2407	-1044	1.84	1.385
Fe	120333	78410	41717	2.96	6.65
K	479755	312613	2056354	14.72	715
Mg	97403	63469	136068	6.50	80
Mn	8844	5763	56637	21.02	21.151
Na	261370	170311	428225	7.51	135
Ni	967	630	1085	5.89	0.473
P	51389	33485	134259	10.10	37
Pb	1070	697	-263	1.51	0.171
S	328401	213989	333980	5.76	210
Sb	139	91	-3	2.58	0.051
Sr	1293	843	2371	7.99	1.2
V	1728	1126	1226	4.66	0.158
U	4	3	2	3.48	0.00074
Zn	44037	28695	-15730	1.75	16.609

D indicates dry deposition, C indicates canopy interaction

EF is canopy enrichment factor

[M] indicates the average concenration of the element or isotope in throughfall precipitation